

Machine learning phases of an Abelian gauge theory

Jhao-Hong Peng

*Department of Physics, Box 90305, Duke University, Durham, NC 27708, USA and
Department of Physics, National Taiwan Normal University, 88, Sec.4, Ting-Chou Rd., Taipei 116, Taiwan*

Yuan-Heng Tseng and Fu-Jiun Jiang*

Department of Physics, National Taiwan Normal University, 88, Sec.4, Ting-Chou Rd., Taipei 116, Taiwan

The phase transition of the two-dimensional $U(1)$ quantum link model on the triangular lattice is investigated by employing a supervised neural network (NN) consisting of only one input layer, one hidden layer of two neurons, and one output layer. No information on the studied model is used when the NN training is conducted. Instead, two artificially made configurations are considered as the training set. Interestingly, the obtained NN not only estimates the critical point accurately but also uncovers the physics correctly. The results presented here imply that a supervised NN, which has a very simple architecture and is trained without any input from the investigated model, can identify the targeted phase structure with high precision.

I. INTRODUCTION

Machine learning (ML) has attracted much attention in the physics community recently. Many ML techniques have been applied to study physics systems and these applications have reached various degrees of success [1–39]. For instance, the methods of neural networks (NN) are demonstrated to be able to identify phases of matter with high accuracy [6, 10–15, 18, 19, 24, 26, 27, 29–31, 38].

Conventionally, one needs to train a NN with certain information about the targeted system in order to carry out a NN study of the associated phase transition. Apart from using relevant physical quantities for the training, the NN considered for such kind of investigation typically has a very complicated architecture. As a result, it takes a huge amount of computing resources to adopt the NN approach to study a phase transition. Because of this, the applications of NN are limited, in particular, to systems of small sizes.

Under such a situation, it is of little motivation to use NN instead of the traditional methods when phase transitions are concerned. Unless certain drawbacks of NN approaches are overcome, NN is hindered from being widely adopted in reality.

In Ref. [39], an autoencoder (AE) and a generative adversarial network (GAN) have been constructed. In particular, each of these two unsupervised NN consists of only one input layer, one hidden layer of 2 neurons, and one output layer. Moreover, these two unsupervised NNs are trained on a one-dimensional (1D) lattice of 200 sites and the training set is composed of two artificially made configurations. It has been shown that these two unsupervised NN successfully estimate the critical points of the three-dimensional (3D) classical $O(3)$ model, the two-dimensional (2D) generalized XY model, the 2D ferromagnetic Potts model, and the 1D Bose-Hubbard model

with high precision. A benchmark calculation indicates that a factor of few thousand in the speed of calculation is gained for the unconventional AE and GANs when they are compared with the performance of the standard NN. A similar idea has been applied to supervised NN as well [38].

In this study, we build a supervised NN made up of one input layer, one hidden layer of two neurons, and one output layer. In addition, we train the supervised NN on a 1D lattice of 200 sites and use two artificially made configurations as the training set. The training process takes only 24 seconds. The constructed NN is then employed to study the phase structure of the 2D $U(1)$ quantum link model, which is an Abelian gauge theory, on the triangular lattice.

The quantum link models are generalizations of the Wilson lattice gauge theory [40–44]. In addition to serving as a regularization of quantum chromodynamics (QCD), these models have very rich physical phenomena such as the splitting of confining strings into individual strands carrying fractionalized electric flux [45–47].

The spontaneous symmetry breaking patterns of the 2D $U(1)$ quantum link model on the triangular lattice before and beyond the phase transition are nontrivial. In other words, the model has an exotic type of phase transition [47]. As a result, it will be intriguing to examine whether the employed NN, which is trained without any input from the targeted model, can identify the physics of the considered system correctly.

Interestingly, although the employed supervised NN has only one hidden layer of 2 neurons and is trained without any information of the considered model, it has determined the associated critical point accurately. Moreover, for both phases, the used NN correctly predicts whether the sublattices are ordered or disordered. This is remarkable because the NN does not know anything about the studied model. The outcomes shown here as well as that in Refs. [38, 39] strongly suggest that training with the input of the considered system is not necessary for a NN to be able to distinguish various

*fjjiang@ntnu.edu.tw

phases. In particular, NNs trained with two artificial configurations, such as the one presented here and those in Refs. [38, 39], are universal since they can be applied to determine the critical points of many models successfully.

The rest of the paper is organized as follows. After the introduction, the 2D $U(1)$ quantum link model and the employed NN are introduced briefly in Secs. II and III, respectively. The NN outcomes are presented in Sec. IV. We conclude our investigation in Sec. V.

II. THE CONSIDERED MODEL

The Hamiltonian of the $U(1)$ quantum link model on the triangular lattice takes the form

$$H = \sum_{\Delta} H_{\Delta} = -J \sum_{\Delta} \left[U_{\Delta} + U_{\Delta}^{\dagger} - \lambda (U_{\Delta} + U_{\Delta}^{\dagger})^2 \right], \quad (1)$$

where $U_{\Delta} = U_{x_1 x_2} U_{x_2 x_3} U_{x_3 x_1}$ is an operator associated with the parallel transport around a triangular plaquette Δ . Here the quantum link operator $U_{x_1 x_2}$ connecting nearest-neighbor sites x_1 and x_2 is given by $U_{x_1 x_2} = S_{x_1 x_2}^1 + i S_{x_1 x_2}^2 = S_{x_1 x_2}^+$ with S being a quantum spin. A rhombic lattice of side length L with periodic boundary conditions is considered in our study, see fig. 1. Notice the rhombic lattice consists of two sublattices A and B . In addition to the $U(1)$ gauge symmetry, the system has several global symmetries such as lattice translations and reflection on a lattice axis as well.

Instead of working directly with the variable of links, we consider the dual degrees of freedom, namely the quantum height variables. The height variables live on the center of triangular plaquette and can take values of $+1$ or -1 .

The construction of a height configuration and its relation to the original flux configuration is detailed in Ref. [47]. Since we are interested in uncovering the relevant physics solely from the NN data without consulting any information about the original system, here we will not go into the details of the studied model and will only briefly summarize the physics and the associated phase structure of the system.

By setting $J = 1$ and varying λ in Eq. 1, there exists a critical value λ_c where a phase transition occurs. The λ_c is estimated to be ~ -0.2150 in Ref. [47]. For $\lambda > \lambda_c$, one of the two sublattices is ordered, implying the 60 degrees rotation O is broken. When $\lambda < \lambda_c$, the charge conjugation C is additionally broken, leading to the case that both sublattices are ordered. The translation symmetry remains unbroken in both the regions of $\lambda > \lambda_c$ and $\lambda < \lambda_c$. Consequently, one has two different nematic phases. The mentioned phase transition is an exotic weak first-order transition as demonstrated in Ref. [47].

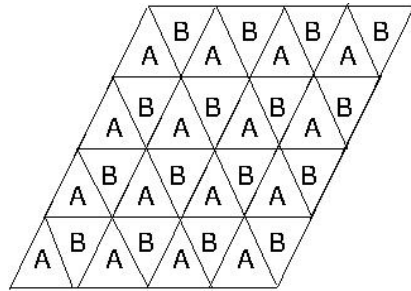


FIG. 1: The rhombic lattice considered in our study. The rhombic lattice consists of two sublattices A and B .

III. THE EMPLOYED NN

The 1D (supervised) NN employed here is built with Keras and Tensorflow [48, 49]. In particular, it is a multi-layer perceptron (MLP) which consists of only one input layer, one hidden layer of 2 neurons, and one output layer.

Since we want to construct a supervised NN without using any information from the considered model, the training set employed here consists of 200 copies of two artificially made one-dimensional (1D) lattices of 200 sites. Particularly, all the sites of one configuration take 1 as their values, and each element of the other (configuration) is 0. Because the training set contains only two types of configurations, it is natural to use $(1, 0)$ and $(0, 1)$ as the output labels.

The algorithm and optimizer employed in training the NN are minibatch and adam (the associated learning rate is set to 0.05), respectively. Moreover, activation functions ReLU and softmax are used in the hidden and output layers, respectively. L_2 regularization is used to avoid overfitting. The steps of one-hot encoding and flattening are considered as well. The loss function utilized is categorical crossentropy. Finally, 800 epochs are conducted and the used batch size is 40.

A short explanation of the NN terminologies mentioned here as well as the details of the training and testing processes are available in Ref. [31, 38]. A cartoon representation of the employed NN is depicted in fig. 2.

IV. THE NN RESULTS

We have carried out large-scale quantum Monte Carlo simulations and prepared few to a few thousand height configurations with various system sizes L and different values of λ . The simulations are done using the algorithm introduced in Ref. [47]. These height configurations will be used for the testing (prediction) stage. In particular, for each height configuration, 200 height variables are chosen randomly to build a configuration that is then considered for the NN prediction.

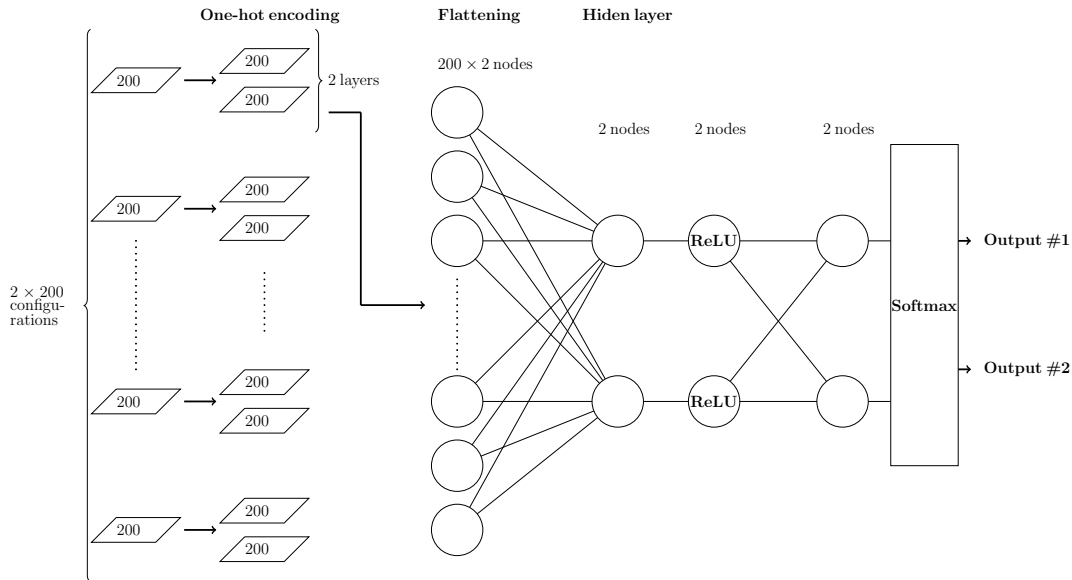


FIG. 2: The supervised neural network considered in this study.

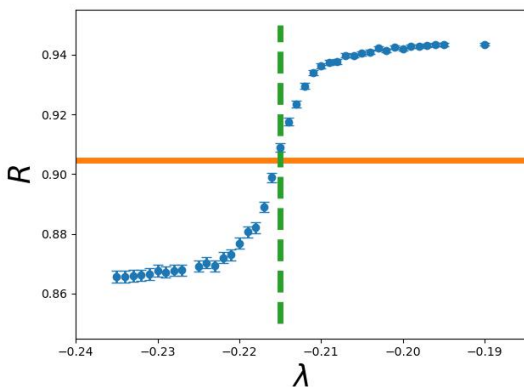


FIG. 3: R as a function of λ for $L = 24$. The vertical dashed line represents the true λ_c . The λ associated with the intersection of the horizontal line and the data of R is the estimated value of λ_c .

A. The determination of λ_c

The magnitude R of the NN outputs is investigated. First of all, we would like to examine whether the quantity R can be employed to estimate the critical point.

R as a function of λ for $L = 24$ is shown in fig. 3. By investigating R over various values of λ , we find that close to λ_c there is a narrow region Λ in λ where the magnitude of R has a dramatic jump. Such a region can be interpreted as the critical region. In addition, the R associated with those λ away from the narrow region saturate to certain constants. Let the saturation values for $\lambda > \Lambda$ and $\lambda < \Lambda$ be denoted by R_R and R_L respectively. Moreover, one defines R_M to be $(R_R + R_L)/2$ (R_M is the horizontal solid line in fig. 3). Then the λ corresponding to the intersection of the horizontal line and the curve of R in fig. 3 matches very well with the critical point $\lambda_c \sim -0.2150$ (the vertical dashed line in fig. 3). This result indicates that such a simple procedure of computing

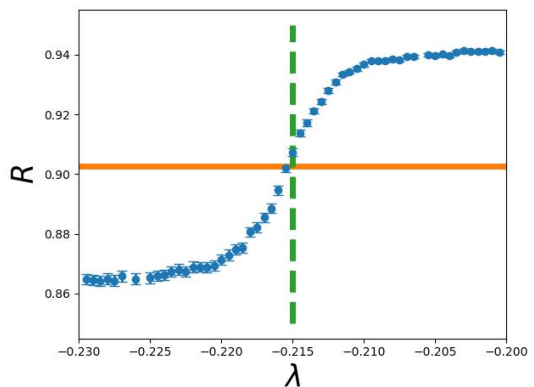


FIG. 4: R as a function of λ for $L = 32$. The vertical dashed line represents the true λ_c . The λ associated with the intersection of the horizontal line and the data of R is the estimated value of λ_c .

can lead to a quite precise estimation of λ_c . This strategy also works for the data of $L = 32$, see fig. 4 and the related caption. To conclude, for sufficiently large system sizes, the procedure of computing the intersection introduced above can be employed to determine the critical point with reasonable high precision.

B. The histograms of R

After presenting a method of calculating λ_c , we want to investigate what information the data of R can reveal. It should be pointed out that in theory the largest and smallest possible values of R are given by 1 (When all the height variables take the same value) and $1/\sqrt{2}$ (When the values of height variables are random), respectively.

The histogram of R for $\lambda = -0.235 < \lambda_c$ and $L = 24$ is shown in the left panel of fig. 5, which has a two peaks structure. In particular, the peaks are located at 1 and

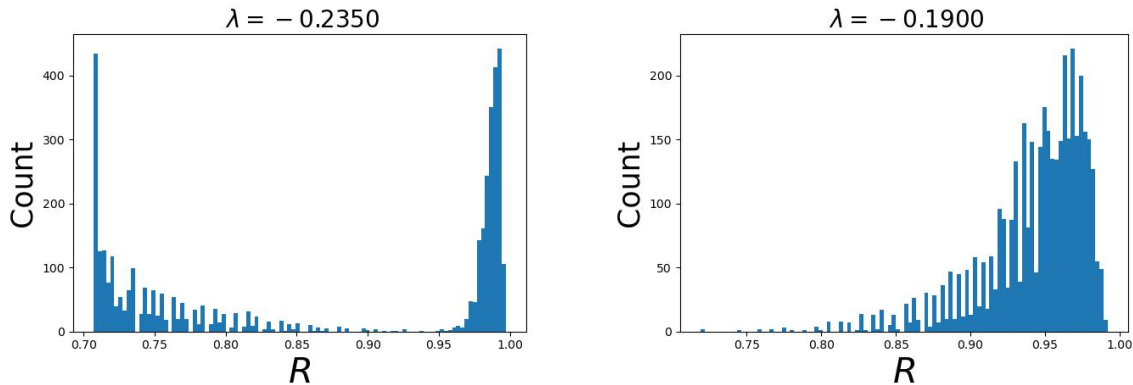


FIG. 5: The histograms of R for $\lambda = -0.235$ (left) and $\lambda = -0.19$ (right).

$1/\sqrt{2}$. Let us consider two types of configurations. The first one is that all the chosen height variables have the same value. The second one is that half of the picked height variables have the value of 1 (-1) and the other half take -1 (1) as their values. The former and the later type of configurations will lead to $R = 1$ and $R = 1/\sqrt{2}$, respectively. To obtain the result shown in the left panel of fig. 5, these two types of configurations should occur with equal probability. In terms of physics, the most probable situation that would result in such an outcome is that the whole height variables can be put into two categories (i.e. the underlying lattice is divided into two sublattices) and each of these two categories is ordered. In other words, certain symmetry is broken spontaneously in both sublattices.

The histogram of R for $\lambda = -0.19 > \lambda_c$ and $L = 24$ is demonstrated in the right panel of fig. 5. The data of R accumulate at the right-hand part of fig. 5. This implies that the number of height variables having a particular value is larger than the number of height variables taking the other value. If one adopts the view of dividing the underlying lattices into two sublattices, then this result can be understood as one sublattice being ordered and the other being disordered. In particular, certain symmetry is broken spontaneously in one sublattice.

Based on the outcomes shown in figs. 3, 4, 5, one concludes that the investigated system has two sublattices A and B . This is in agreement with fig. 1 which indeed has two sublattices. In other words, one can obtain the correct features of the studied model solely from the R of the NN outputs. In particular, the NN is trained without any input from the system.

C. The running histories of R

Having estimated the location of λ_c and understood certain symmetry-breaking patterns of the system, we now turn to explore the running histories of R on sublattices A and B .

The running histories of R on sublattice A for $\lambda = -0.19, -0.215$, and -0.235 on a 24 by 24 lattice are

shown as the left, middle, and right panels of fig. 6, respectively. These results imply that the sublattice A is ordered for both the regions of $\lambda > \lambda_c$ and $\lambda < \lambda_c$. In addition, the running history of R at -0.215 (which is the expected λ_c) shows a tunneling between $R = 1$ and $R = 1/\sqrt{2}$. This is a feature of a first-order phase transition. Similarly, The running histories of R on sublattice B demonstrated in fig. 7 indicate that sublattice B is ordered for $\lambda < \lambda_c$ and disordered for $\lambda > \lambda_c$. In particular, the middle panel of fig. 7 also shows a signal of first-order phase transition. In other words, both sublattices A and B reveal the fact that the phase transition is first order. Here we would like to point out that with the traditional Monte Carlo approach, the first-order signal appears only when the system sizes are sufficiently large ($L \geq 48, 64$). For the NN calculations, one obtains the correct conclusion regarding the nature of the phase transition from the outcomes of $L = 24$.

V. DISCUSSIONS AND CONCLUSIONS

In this study, we investigate the phase transition of the 2D $U(1)$ quantum link model on the triangular lattice using the method of NN. The employed NN has only one hidden layer of two neurons and is trained without any input from the considered model. Because of this set up, the training process takes only 24 seconds on a server with two opteron 6344 and 96G memory.

Despite its simplicity, with the magnitude R of the output, the constructed NN not only determines the critical λ_c precisely, it also identifies the physics before and beyond the transition correctly. These conclusions are obtained solely from the NN data without consulting any information about the investigated model.

The conventional NNs used to study phase transitions are typically made up of several layers and each layer has many neurons. Such a NN architecture leads to a lot of tunable parameters, hence the corresponding training is very time-consuming. Intuitively, the idea of considering complicated deep learning NN is that the studied systems have huge amounts of degrees of freedom, therefore one

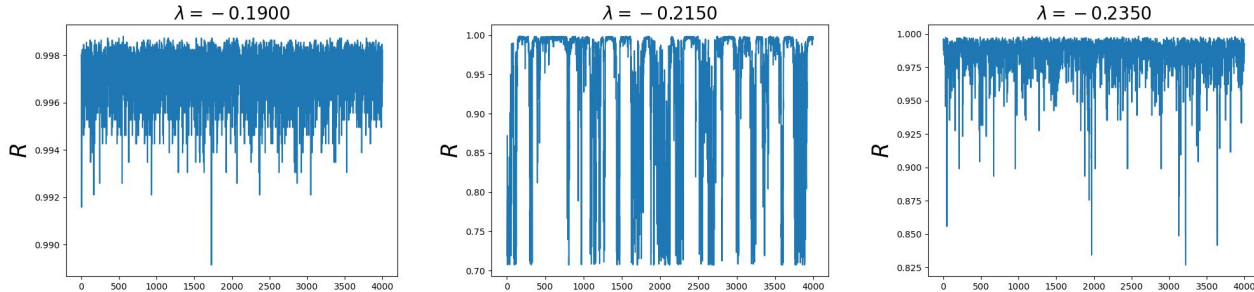


FIG. 6: The running histories of R of sublattice A for $\lambda = -0.19$ (left), $\lambda = -0.215$ (middle), and $\lambda = -0.235$ (right).

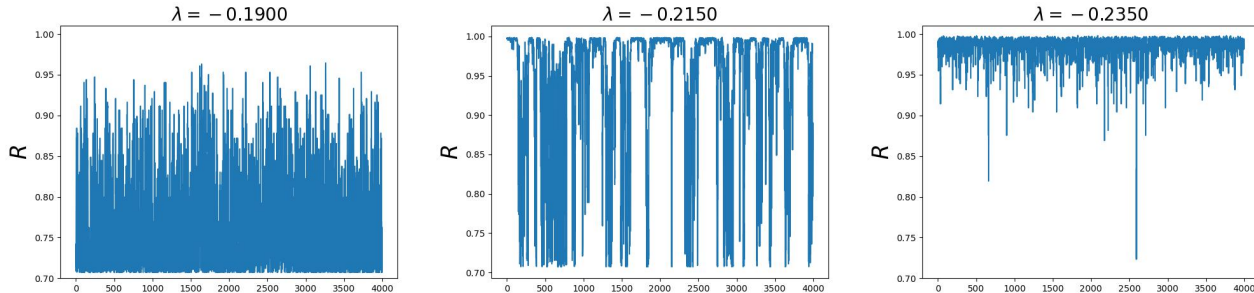


FIG. 7: The running histories of R of sublattice B for $\lambda = -0.19$ (left), $\lambda = -0.215$ (middle), and $\lambda = -0.235$ (right).

needs to tune many NN parameters in order to capture the right physics. Our investigation as well as that in Ref. [39] suggest that one hidden layer having two neurons is sufficient to uncover the phase structures of many nontrivial models.

To promote the adoption of NN techniques in real calculations, the NNs definitely should have some advantage that makes NNs outperform the traditional approaches. When phase transition is concerned, the conventional NNs considered in the literature require quite a lot of computing efforts. It is then not so promising to use NN instead of the traditional methods to perform the needed calculations. The unconventional NN strategy shown here uses only several minutes to complete the

whole calculation (from the training to the prediction). As a result, it offers an efficient alternative to the traditional approaches when phase transitions are studied.

Finally, similar to the unsupervised AE and GAN of Ref. [39], the supervised NN considered here can directly apply to other models without performing any new training.

Acknowledgement

Partial support from National Science and Technology Council (NSTC) of Taiwan is acknowledged.

-
- [1] Matthias Rupp, Alexandre Tkatchenko, Klaus-Robert Müller, and O. Anatole von Lilienfeld, *Fast and Accurate Modeling of Molecular Atomization Energies with Machine Learning*, Phys. Rev. Lett. **108** 058301 (2012).
- [2] John C. Snyder, Matthias Rupp, Katja Hansen, Klaus-Robert Müller, and Kieron Burke, *Finding Density Functionals with Machine Learning*, Phys. Rev. Lett. **108** 253002 (2012).
- [3] P. Baldi, P. Sadowski and D. Whiteson, *Enhanced Higgs Boson to $\tau^+\tau^-$ Search with Deep Learning*, Phys. Rev. Lett. **114**, 111801 (2015).
- [4] V. Mnih, K. Kavukcuoglu, D. Silver, A. A. Rusu, J. Veness, M. G. Bellemare, A. Graves, M. Riedmiller, A. K. Fidjeland, G. Ostrovski, S. Petersen, C. Beattie, A. Sadik, I. Antonoglou, H. King, D. Kumaran, D. Wierstra, S. Legg and D. Hassabis, *Human-level control through deep reinforcement learning*, Nature **518**, no.7540, 529-533 (2015).
- [5] J. Searcy, L. Huang, M. A. Pleier and J. Zhu, *Determination of the WW polarization fractions in $pp \rightarrow W^\pm W^\pm jj$ using a deep machine learning technique*, Phys. Rev. D **93**, no.9, 094033 (2016).
- [6] Tomoki Ohtsuki and Tomi Ohtsuki, *Deep Learning the Quantum Phase Transitions in Random Two-Dimensional Electron Systems*, J. Phys. Soc. Jpn. **85**, 123706 (2016).
- [7] M. Attarian Shandiz and R. Gauvin, *Application of machine learning methods for the prediction of crystal system of cathode materials in lithium-ion batteries*, Computational Materials Science **117** (2016) 270-278.
- [8] B. Hoyle, *Measuring photometric redshifts using galaxy images and Deep Neural Networks*, Astron. Comput. **16**, 34-40 (2016).
- [9] A. Mott, J. Job, J. R. Vlimant, D. Lidar and M. Spiropulu, *Solving a Higgs optimization problem with quantum annealing for machine learning*, Nature **550**, no.7676,

- 375-379 (2017).
- [10] Juan Carrasquilla, Roger G. Melko, *Machine learning phases of matter*, Nature Physics **13**, 431–434 (2017).
- [11] Akinori Tanaka, Akio Tomiya, *Detection of Phase Transition via Convolutional Neural Networks*, J. Phys. Soc. Jpn. **86**, 063001 (2017).
- [12] Evert P.L. van Nieuwenburg, Ye-Hua Liu, Sebastian D. Huber, *Learning phase transitions by confusion*, Nature Physics **13**, 435–439 (2017).
- [13] Dong-Ling Deng, Xiaopeng Li, and S. Das Sarma, *Machine learning topological states*, Phys. Rev. B **96** 195145 (2017).
- [14] Yi Zhang, Roger G. Melko, and Eun-Ah Kim *Machine learning Z_2 quantum spin liquids with quasiparticle statistics*. Phys. Rev. B **96**, 245119 (2017).
- [15] Wenjian Hu, Rajiv R. P. Singh, and Richard T. Scalettar, *Discovering phases, phase transitions, and crossovers through unsupervised machine learning: A critical examination*, Phys. Rev. E **95**, 062122 (2017).
- [16] J. Tubiana and R. Monasson, *Emergence of Compositional Representations in Restricted Boltzmann Machines*, Phys. Rev. Lett. **118**, 138301 (2017).
- [17] Kolb, B., Lentz, L. C. and Kolpak, A. M., *Discovering charge density functionals and structure-property relationships with PROPhet: A general framework for coupling machine learning and first-principles methods*, Sci Rep **7**, 1192 (2017).
- [18] C.-D. Li, D.-R. Tan, and F.-J. Jiang, *Applications of neural networks to the studies of phase transitions of two-dimensional Potts models*, Annals of Physics, 391 (2018) 312-331.
- [19] Kelvin Ch'ng, Nick Vazquez, and Ehsan Khatami, *Unsupervised machine learning account of magnetic transitions in the Hubbard model*, Phys. Rev. E **97**, 013306 (2018).
- [20] Lu, S., Zhou, Q., Ouyang, Y. et al., *Accelerated discovery of stable lead-free hybrid organic-inorganic perovskites via machine learning*, Nat Commun **9**, 3405 (2018).
- [21] Keith T. Butler, Daniel W. Davies, Hugh Cartwright, Olexandr Isayev, and Aron Walsh, *Machine learning for molecular and materials science*, Nature **559**, 547–555 (2018).
- [22] L. G. Pang, K. Zhou, N. Su, H. Petersen, H. Stöcker and X. N. Wang, *An equation-of-state-meter of quantum chromodynamics transition from deep learning*, Nature Commun. **9**, no.1, 210 (2018).
- [23] Phiala E. Shanahan, Daniel Trewartha, and William Detmold, *Machine learning action parameters in lattice quantum chromodynamics*, Phys. Rev. D **97**, 094506 (2018).
- [24] Joaquin F. Rodriguez-Nieva and Mathias S. Scheurer, *Identifying topological order through unsupervised machine learning*, Nat. Phys. **15**, 790–795 (2019).
- [25] M. Cavaglia, K. Staats and T. Gill, *Finding the origin of noise transients in LIGO data with machine learning*, Commun. Comput. Phys. **25**, no.4, 963-987 (2019).
- [26] Wanzhou Zhang, Jiayu Liu, and Tzu-Chieh Wei, *Machine learning of phase transitions in the percolation and XY models*, Phys. Rev. E **99**, 032142 (2019).
- [27] Xiao-Yu Dong, Frank Pollmann, and Xue-Feng Zhang, *Machine learning of quantum phase transitions*, Phys. Rev. B **99**, 121104(R) (2019).
- [28] G. P. Conangla, F. Ricci, M. T. Cuairan, A. W. Schell, N. Meyer and R. Quidant, *Optimal Feedback Cooling of a Charged Levitated Nanoparticle with Adaptive Control*, Phys. Rev. Lett. **122**, 223602 (2019).
- [29] D.-R. Tan *et al.* *A comprehensive neural networks study of the phase transitions of Potts model*, 2020 New J. Phys. **22** 063016.
- [30] A. Lidiak and Z. Gong, *Unsupervised Machine Learning of Quantum Phase Transitions Using Diffusion Maps*, Phys. Rev. Lett. **125**, no.22, 225701 (2020).
- [31] D.-R. Tan and F.-J. Jiang, *Machine learning phases and criticalities without using real data for training*, Phys. Rev. B **102**, 224434 (2020).
- [32] R. J. Shalloo, S. J. D. Dann, J. N. Gruse, C. I. D. Underwood, A. F. Antoine, C. Arran, M. Backhouse, C. D. Baird, M. D. Balcazar and N. Bourgeois, *et al.* *Automation and control of laser wakefield accelerators using Bayesian optimization*, Nature Commun. **11**, no.1, 6355 (2020).
- [33] R. M. Geilhufe and B. Olsthoorn, *Identification of strongly interacting organic semimetals*, Phys. Rev. B **102**, no.20, 205134 (2020).
- [34] A. J. Larkoski, I. Moulton and B. Nachman, *Jet Substructure at the Large Hadron Collider: A Review of Recent Advances in Theory and Machine Learning*, Phys. Rept. **841**, 1-63 (2020).
- [35] G. Aad *et al.* [ATLAS], *Dijet resonance search with weak supervision using $\sqrt{s} = 13$ TeV pp collisions in the ATLAS detector*, Phys. Rev. Lett. **125**, no.13, 131801 (2020).
- [36] R. Morgan *et al.* [DES], *Constraints on the Physical Properties of GW190814 through Simulations Based on DECAM Follow-up Observations by the Dark Energy Survey*, Astrophys. J. **901**, no.1, 83 (2020).
- [37] K. A. Nicoli, C. J. Anders, L. Funcke, T. Hartung, K. Jansen, P. Kessel, S. Nakajima and P. Stornati, *Estimation of Thermodynamic Observables in Lattice Field Theories with Deep Generative Models*, Phys. Rev. Lett. **126**, no.3, 032001 (2021).
- [38] D.-R. Tan, J.-H. Peng, Y.-H. Tseng, F.-J. Jiang, *A universal neural network for learning phases*, Eur. Phys. J. Plus **136** (2021) 11, 1116.
- [39] Yuan-Heng Tseng, Fu-Jiun Jiang, and C.-Y. Huang, *A universal training scheme and the resulting universality for machine learning phases*, PTEP, in press.
- [40] K. G. Wilson, *Confinement of quarks*, Phys. Rev. D **10**, 2445 (1974).
- [41] D. Horn, *Finite matrix models with continuous local gauge invariance*, Phys. Lett. **B 100**, 149 (1981).
- [42] P. Orland and D. Rohrlich, *Lattice gauge magnets: Local isospin from spin*, Nucl. Phys. **B 338**, 647 (1990).
- [43] S. Chandrasekharan and U.-J. Wiese, *Quantum link models: A Discrete approach to gauge theories*, Nucl. Phys. B **492**, 455 (1997).
- [44] R. Brower, S. Chandrasekharan, and U.-J. Wiese, *QCD as a quantum link model*, Phys. Rev. D **60**, 094502 (1999).
- [45] D. Banerjee, F.-J. Jiang, P. Widmer, and U.-J. Wiese, *The $(2 + 1)$ -d $U(1)$ quantum link model masquerading as deconfined criticality*, J. Stat. Mech., P12010 (2013).
- [46] D. Banerjee, F.-J. Jiang, T. Z. Olesen, P. Orland, and U.-J. Wiese, *From the $SU(2)$ quantum link model on the honeycomb lattice to the quantum dimer model on the kagome lattice: Phase transition and fractionalized flux strings*, Phys. Rev. B **97**, 205108 (2018).
- [47] D. Banerjee, S. Caspar, F.-J. Jiang, J.-H. Peng, and U.-J. Wiese, *Nematic confined phases in the $U(1)$ quantum*

link model on a triangular lattice: Near-term quantum computations of string dynamics on a chip, Phys. Rev. Res. **4**, 023176 (2022).

[48] <https://keras.io>

[49] <https://www.tensorflow.org>